Eur. Phys. J. Special Topics **225**, 1017–1035 (2016)

DOI: 10.1140/epjst/e2016-02652-5

THE EUROPEAN PHYSICAL JOURNAL SPECIAL TOPICS

Review

From mechanical to biological oscillator networks: The role of long range interactions

T. Bountis[1,2,a]

[1] Center for Research and Applications of Nonlinear Systems, University of Patras, 26500 Patras, Greece
[2] Department of Mathematics, Nazarbayev University, Kabanbay batyr Ave. 53, Astana 010000, Republic of Kazhakstan

Received 28 March 2016 / Received in final form 26 July 2016
Published online 30 September 2016

Abstract. The study of one-dimensional particle networks of Classical Mechanics, through Hamiltonian models, has taught us a lot about oscillations of particles coupled to each other by nearest neighbor (short range) interactions. Recently, however, a careful analysis of the role of *long range interactions* (LRI) has shown that several widely accepted notions concerning chaos and the approach to thermal equilibrium need to be modified, since LRI strongly affects the *statistics* of certain very interesting, long lasting metastable states. On the other hand, when LRI (in the form of non-local or all-to-all coupling) was introduced in systems of biological oscillators, Kuramoto's theory of synchronization was developed and soon thereafter researchers studied amplitude and phase oscillations in networks of FitzHugh Nagumo and Hindmarsh Rose (HR) neuron models. In these models certain fascinating phenomena called *chimera states* were discovered where populations of synchronous and asynchronous oscillators are seen to coexist in the same system. Currently, their synchronization properties are being widely investigated in HR mathematical models as well as realistic neural networks, similar to what one finds in simple living organisms like the *C.elegans* worm.

1 Introduction

1.1 Long range interactions in mechanical oscillators

As is well-known, many problems in theoretical physics are expressed in the form of Hamiltonian systems. Of these the first to be extensively studied were low-dimensional, possessing as few as two (or three) degrees of freedom [1]. In the last 20 years, however, great attention has been devoted to Hamiltonian systems of *high dimensionality*. Among these perhaps the most famous are those that deal with the

[a] e-mail: tassos50@otenet.gr

dynamics and statistics of a large number N of mass particles coupled to each other by nearest neighbor interactions [2]. In such systems, certain *local* phenomena like the "stickiness" of chaotic orbits near tori of regular motion gave rise to important questions concerning the system's *global* behavior in the long time limit, at moderate values of N and total energy E. In particular, long-lasting quasi-stationary states (QSS) were discovered, which may be termed "weakly chaotic" since they are described by probability density functions (pdfs) which are *significantly different* than the purely Gaussian pdfs associated with Boltzmann Gibbs (BG) ergodicity, or "strong chaos" [3,4].

Realizing that such metastable phenomena are due to long-tail correlations and intrinsic interactions of longer range than had been expected, a number of researchers decided to introduce long range interactions (LRI) *explicitly* into the Hamiltonian and study the dynamics in the thermodynamic limit, where $E \to \infty$ and $N \to \infty$ with $E/N =$ constant [5–12]. Perhaps the best known example in this class is the so-called Hamiltonian Mean Field model, where the Maximal Lyapunov Exponent (MLE) was shown to decrease with increasing number of degrees of freedom N, according to a specific power law [6,7,10,11]. This signified that, at least in that model, a more organized "global" behavior appears to exist, which has important implications regarding the thermodynamics of the system.

More recently, another famous example in this category, the Fermi Pasta Ulam (FPU) 1-dimensional lattice of N nonlinearly coupled oscillators was studied in the presence of long range interactions [13]. The Hamiltonian of this system may be written in the general form

$$\mathcal{H}(p,x) = \frac{1}{2}\sum_{n=1}^{N} p_n^2 + \sum_{n=0}^{N} V_2(x_{n+1}-x_n) + \sum_{n=0}^{N} V_4(x_{n+1}-x_n), \tag{1}$$

with V_2 and V_4 representing the quadratic and quartic functions $V_2(u) = au^2/2$ and $V_4(u) = bu^4/4$ under purely nearest-neighbor interactions. The p_n, x_n are the canonical conjugate pairs of momentum and position variables assigned to the n^{th} particle, with $n = 1, 2, ..., N$ and fixed boundary conditions, i.e. $x_0 = x_{N+1} = p_0 = p_{N+1} = 0$.

Let us now modify the above form of the FPU Hamiltonian by allowing interactions among *all* particles in the V_2 and V_4 parts of the potential with coefficients that decay with distance as $1/r^{\alpha_1}$ and $1/r^{\alpha_2}$ respectively. In particular, the Hamiltonian that describes this generalized FPU β-model has the form

$$\begin{aligned}\mathcal{H} = & \frac{1}{2}\sum_{n=1}^{N} p_n^2 + \frac{a}{2\widetilde{N}_1}\sum_{n=0}^{N}\sum_{m=n+1}^{N+1}\frac{(x_n-x_m)^2}{(m-n)^{\alpha_1}} \\ & + \frac{b}{4\widetilde{N}_2}\sum_{n=0}^{N}\sum_{m=n+1}^{N+1}\frac{(x_n-x_m)^4}{(m-n)^{\alpha_2}},\end{aligned} \tag{2}$$

where a and b are positive constants. Note that the rescaling factors $\widetilde{N}_i$, $i = 1, 2$ in (2)

$$\widetilde{N}_i(N,\alpha_i) \equiv \frac{1}{N}\sum_{n=0}^{N}\sum_{m=n+1}^{N+1}\frac{1}{(m-n)^{\alpha_i}}, \quad (i=1,2) \tag{3}$$

serve to make the Hamiltonian *extensive*, i.e. proportional to N. Indeed, without them the sums of V_2 and V_4 in (2) would increase as $(N+1)(N+2)/2$ in the thermodynamic limit, while the kinetic energy grows like N [13]. Notice that $\widetilde{N}_i \simeq 1$ when $\alpha_i \to \infty$, which, in the $N \to \infty$ limit, reduces Hamiltonian (2) to (1).

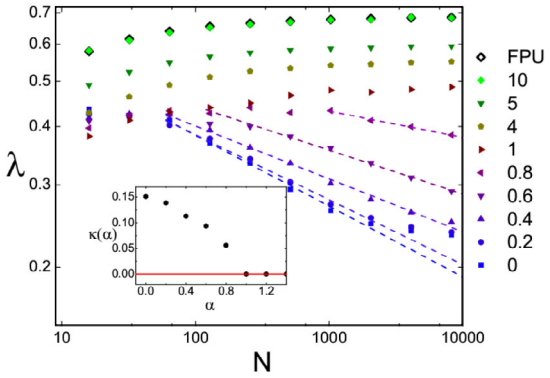

Fig. 1. The Maximal Lyapunov Exponent $MLE = \lambda$ versus the size N, for various $\alpha = \alpha_2$ values and $\alpha_1 = \infty$ in (2). We have set $\varepsilon = 9$, $b = 10$ and fixed boundary conditions. (Figure taken from [13].)

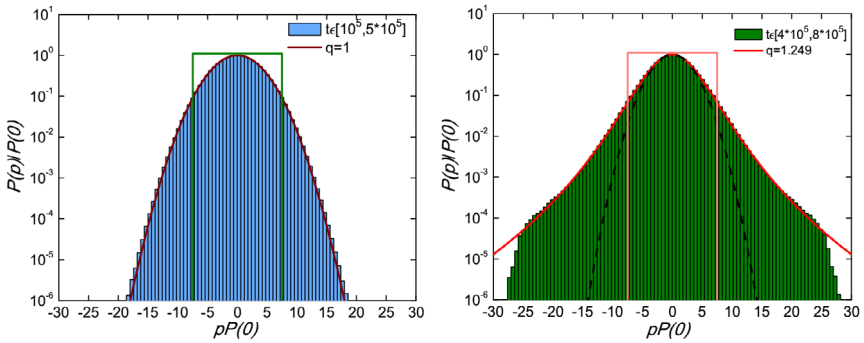

Fig. 2. Time-averaged momentum distributions for the system (2) with $\alpha = \alpha_2$, $\alpha_1 = \infty$, $\varepsilon = 9$, $b = 10$ and $N = 8192$: Top figure corresponds to $\alpha = 1.4$ and bottom figure to $\alpha = 0.7$. (Figure taken from [13].)

The parameters α_1 and α_2 control the range of interactions and play a crucial role in the dynamics of the system. In fact, if we set $\alpha_1 = \infty$ and $\alpha_2 = \alpha$, it was shown in [13] that the MLE λ displays a crossover at the value $\alpha = 1$ below which λ starts to decrease towards zero as N increases. This is shown in Fig. 1 (in double logarithmic scale for several values of α), where λ is seen to decay vs. N by a power law for $\alpha < 1$, while it appears to converge to a positive value for $\alpha \geq 1$. The calculations presented here have been made keeping the specific energy $\varepsilon = 9$ fixed.

Observe that Fig. 1 provides strong evidence of a *transition* from strong to weak chaos, when the interactions decay as $1/r$ with respect to the inter-particle distance. Now let us explore the implications of LRI regarding the *statistical* behavior of these types of chaotic behavior, with regard to what was referred to above as "strong" vs. "weak" chaos. For this purpose, we will start at $t = 0$ with positions equal to zero and momenta drawn randomly from a uniform distribution and evaluate pdfs of the sums of the the momenta in the spirit of the central limit theorem. Thus, as seen in Fig. 2, we assign to each p_j-interval on the horizontal axis the number of times that the momenta fall in the j-th band, calculated over long time intervals. In Fig. 2 we show two representative examples of such pdfs, one for the case of short range (i.e. $\alpha > 1$) and one for long range interactions (i.e. $\alpha < 1$). The difference in the two pdfs is distinct: For $\alpha > 1$ a Gaussian is quickly formed indicating BG ergodicity and

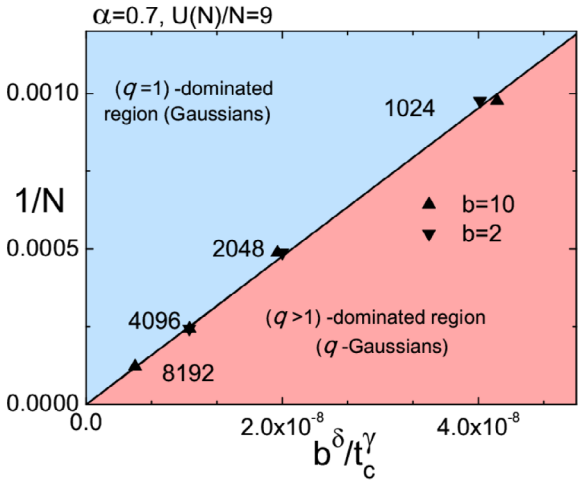

Fig. 3. Crossover boundary between the Gaussian and q-Gaussian regimes, when $N = 1024, 2048, 4096, 8192$ for the systems with $\varepsilon = 9$, and all b values. The fitting straight line is $1/N = Db^{\delta}/t_c^{\gamma}$, with $D = 2.3818 \times 10^4$, $\delta = 0.27048$, and $\gamma = 1.365$. (Figure taken from [13].)

"strong" chaos, while for $\alpha < 1$ the data is well fitted by a q-Gaussian pdf of the form

$$p_q(x) = Ae_q^{-\beta x^2} = A(1 - (1-q)\beta x^2)^{1/(1-q)}, \tag{4}$$

with $q = 1.249$. This pdf maximizes the Tsallis entropy [14]

$$S_q = -k\frac{1 - \sum_{i=1}^{W} p_i^q}{1-q}, \tag{5}$$

under the constraint $\sum_{i=1}^{W} p_i = 1$, where q is the entropic index, β is a free parameter and A a normalization constant. Expression (4) is a generalization of the Gaussian, since in the limit $q \to 1$, $e_q \to e$. The Tsallis entropy is *not additive*, and, in general, *non-extensive* and thus offers the possibility of studying cases whose subsystems are always correlated, as is the situation with many realistic physical systems [14].

The value of q, in fact, reveals how far the system is from thermal equilibrium. It is not generally constant, as it often tends to become 1 (Gaussian pdf) over intervals that correspond to the lifetime of the QSS at hand. Let us denote by $t = t_c$ the time after which q starts decreasing to its BG value ($q = 1$). The transition from the weakly chaotic QSS to ergodicity and Boltzmann's statistics is shown by a schematic diagram in Fig. 3, where a crossover boundary is drawn as a straight line between the Gaussian and q-Gaussian regimes, for $N = 1024, 2048, 4096, 8192$, $\varepsilon = 9$, and all b values. The straight line is given by $1/N = Db^{\delta}/t_c^{\gamma}$, with $D = 2.3818 \times 10^4$, $\delta = 0.27048$, and $\gamma = 1.365$ (see also [13]).

In a recent paper, H. Christodoulidi et al. [15] examined the generalized FPU β–Hamiltonian in the form (2), taking α_1 and α_2 to vary over all allowed values ≥ 0 and obtained a number of interesting results concerning the dynamics and statistics of the system under LRI. Most importantly, they found that in the absence of quadratic terms V_2 and for full LRI on V_4 (i.e. $\alpha_2 = 0$), the system obeys Tsallis statistics and is weakly chaotic in the thermodynamic limit of $t_c \to \infty$ and $N \to \infty$, as the index q in that limit is extrapolated to q_∞ values that are strictly greater than 1. These results are briefly reviewed here in Sect. 2.

1.2 Long range interactions in biological oscillators

About ten years ago, a novel dynamical phenomenon was discovered in populations of identical and symmetrically coupled oscillators: Under non-local coupling that generally decays with distance, a surprising coexistence of synchronized and asynchronous populations was revealed and given the name *chimera state* after the Greek mythological creature made up of different animals.

Chimera states were first reported by Kuramoto and Battogtokh in a model of densely and uniformly distributed oscillators, described by the complex Ginzburg-Landau equation in the weak coupling limit and one spatial dimension, with non-local coupling of exponential form [20]. This was followed by the work of Abrams and Strogatz [21], who observed this phenomenon in a 1-dimensional ring continuum of phase oscillators assuming non-local coupling with a cosine kernel and gave it the name "chimera". The same authors also found chimera states in networks of identical, symmetrically coupled Kuramoto phase oscillators [22] by considering two populations with all-to-all coupling, assuming stronger coupling within each population and weaker coupling between them.

More recently, Laing and co-authors used the same model to demonstrate the presence of chimeras in coupled Stuart-Landau oscillators [27] and investigated the effect of random removal of network connections on the existence and stability of chimera states [28]. Chimeras have also been observed in many other systems, including coupled chaotic logistic maps and Rössler models [29]. The first experimental evidence of such states was subsequently reported in populations of coupled chemical oscillators, as well as optical coupled-map lattices realized by liquid-crystal light modulators [30,31].

Concerning the importance of chimera states in brain dynamics, it is believed that they could potentially explain the phenomenon of unihemispheric sleep observed in birds and dolphins which sleep with one eye open, suggesting that one hemisphere of the brain is synchronous while the other is asynchronous [32,33]. For this reason it is particularly interesting that such states have been recently observed in FitzHugh–Nagumo [34] and Hindmarsh–Rose [24] networks of coupled oscillators modeling neuron dynamics. The results of the latter study are briefly reviewed here in Sect. 3.

Synchronization in phase oscillator systems with an inertial term involving a second order derivative multiplied by a mass parameter $m > 0$ has been theoretically studied by some researchers (see e.g. the review [19]). In some of these works an external periodic driving is included and a Fokker-Planck analysis is performed relating critical behavior and synchronization transitions to those of the corresponding Kuramoto model in the limit $m \to 0$. This raises the interesting question whether chimera states can actually be observed in physical systems of this type.

Recently, this question was answered affirmatively in an experiment involving two populations of identical mechanical metronomes, whose inter-population coupling is weaker than the coupling within each subpopulation [35]. In this setting, chimeras were shown to emerge in a thin region of parameter space as a competition between two fundamental synchronization states. A variety of complex chimera-like states was observed and a mathematical model was proposed with variable damping and all oscillator masses equal to unity.

In the paper [38] Bountis et al. demonstrated the existence of chimera states in two non-locally coupled populations of pendulum-like elements, in which dissipation is modeled by a first derivative term multiplied by a parameter $\epsilon > 0$. As in other studies, the coupling within each population is weaker than the one between the populations. The results of this work are summarized in Sect. 4. Finally, this review ends with our conclusions listed in Sect. 5.

2 LRI in an FPU-β model with quadratic and quartic terms

Analyzing the solutions of the generalized FPU-β Hamiltonian systems (2), Christodoulidi et al. showed in [15] that typical momentum pdfs attain a classical Gaussian shape, either under purely short range interactions, or when LRI apply only to the quadratic part. On the other hand, when LRI applies to the quartic interactions independently of interactions in the quadratic part, a clear q-Gaussian shape emerges, as BG thermodynamics and strong chaos prevail. As is evident from these results, the mechanism of LRI drives the system's behavior away from BG statistics, only if the quartic potential is long range. Instead, when LRI apply *only* to the quadratic part, purely Gaussian pdfs are obtained.

Now, it is interesting to focus on the q values of the model under LRI with different exponents α_1, α_2. What we would like to ask is: How does q change when one applies LRI to the quartic potential and varies only the range of interactions in the quadratic part? As we have mentioned, q-Gaussian distributions are associated with weak chaos and are linked to QSS which persist for very long times, until the system achieves energy equipartition at complete thermalization. In this regard, the precise value of q is very significant since the higher the value of q the more the solution remains at a QSS, as the orbits get trapped for longer and longer times in weakly chaotic regimes of phase space.

Extrapolating the value of q in the limit $N \to \infty$, the authors of [15] estimate the asymptotic value $q = q_\infty$ and also vary α_2 to determine the dependence of q_∞ on the interaction range applied to the quartic part of the potential at the thermodynamic limit. To this end, they consider a given value of $\alpha_2 < 1$ and systematically calculate the q dependence on N. Plotting these q values in Fig. 4(a) versus $1/\log N$ it is shown that their dependence is accurately described by the following expression:

$$q(N, \alpha_2) = q_\infty(\alpha_2) - c(\alpha_2)/\log N, \tag{6}$$

where $c(\alpha_2)$ is some constant.

This is important because it shows that the $q_\infty(\alpha_2)$ obtained from Fig. 4(a) by the intercept of the straight line Eq. (6) with the vertical axis (as $N \to \infty$) is larger than 1, which implies that the q-Gaussians are attractors in that limit. Next, plotting $q_\infty(\alpha_2)$ vs. α_2 in Fig. 4(b), one observes that it starts from 5/3 for $\alpha_2 = 0$, as predicted numerically and theoretically in [14], and then, after about $\alpha_2 = 0.2$, falls linearly towards 1. In particular, for $0.2 \leq \alpha_2 \leq 0.8$ the values of $q_\infty(\alpha_2)$ decrease as $q_\infty(\alpha_2) = 1.79 - 0.475\alpha_2$.

Note that the value of q reaches unity at $\alpha_2 = 1.5$ and not at the expected $\alpha_2 = 1$ threshold between short and long range interactions. This is a very interesting phenomenon that might be explained by the fact that q takes a very long time to converge to 1 over the range $1 \leq \alpha_2 \leq 1.4$. Its precise justification, however, remains open.

A question of central importance in these studies is how long q remains larger than 1. In other words, how long does the system take before it thermalizes? To give an answer we need to extend the results of [13] for different α_2 values. More specifically, in [13] it was found that for an exponent $\alpha_2 = 0.7$ in the quartic part of the potential, the critical time t_c (defined by the intersection of two fitting lines: one representing the initial slow decrease and the other the power law behavior with a bigger slope) at which q starts falling towards one increases with N as $N \propto t_c^\gamma$, for $\gamma \simeq 1.36$. This is a fundamental result because it suggests that t_c becomes infinite only in the thermodynamic limit, where weak chaos in the form of q-statistics changes to BG thermostatistics.

It would be interesting, therefore, to examine this crossover value t_c for various α_2 ranges. To this end, the authors of [15] fixed $N = 16384$, took $a_1 \to \infty$ and plotted in

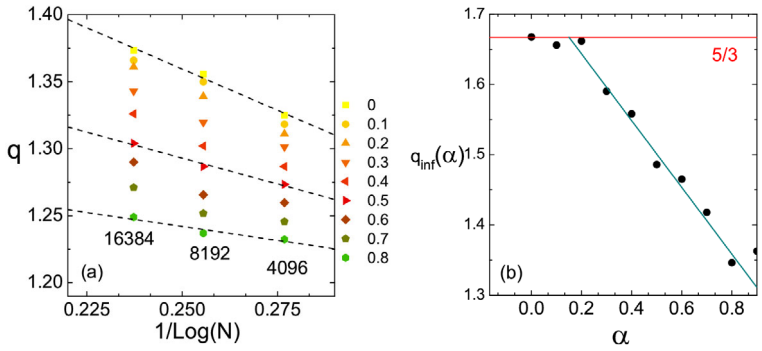

Fig. 4. (a) The linear dependence of q on $1/\log N$ for $N = 4096, 8192, 16384$ depicted here provides an estimate for q_∞ in the thermodynamic limit, as α_2 changes. (b) The values of q_∞ are plotted here versus α_2. Clearly, for α_2 above 1.4, one obtains $q = 1$. (Figures taken from [15].)

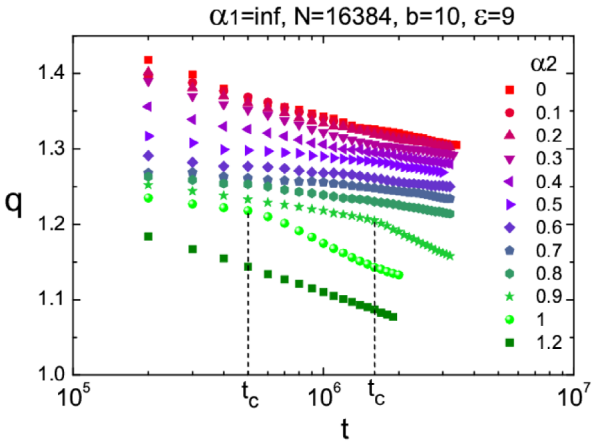

Fig. 5. Evolution of the index q: The plot of q when $N = 16384$ for various α_2 values and $\alpha_1 \to \infty$. The points at which the power laws change slope correspond to the crossover times t_c at which the QSS ends and the approach to BG thermal equilibrium begins. It seems plausible that t_c for very low values of α_2 are too large to be numerically accessible. (Figures taken from [15].)

Fig. 5 q vs. t for different α_2 over this range. As we see in the figure, for small values of α_2, q appears to decrease very slowly, following a power law that forms a single straight line in linear-logarithmic scale (see the top curves in Fig. 5). The shape of the plots shows that as α_2 increases, the initial 'straight line' breaks at some point into a second one that tends faster to $q = 1$. For example, for $\alpha_2 = 0.9$, this crossover point is about $t_c \approx 1.6 \times 10^6$, while at $\alpha_2 = 1$ it becomes as small as $t_c \approx 5 \times 10^5$.

3 Chimera states in networks of HR neuron oscillator models

3.1 Synchronization in complex networks

Synchronization in complex systems occurs when an enormous system of oscillators spontaneously locks to a common frequency, despite the inevitable differences in the

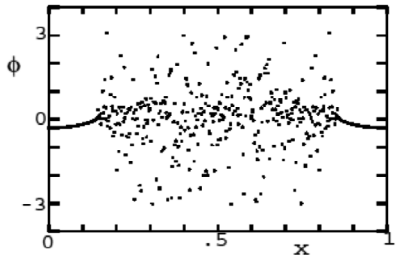

Fig. 6. A time snapshot of the variables $\theta_i(t)$ of the Kuramoto–Battoktokh solution of Eq. (8) showing the chimera state. (Figure taken from [20].)

natural frequencies of the individual oscillators. Synchronization processes are ubiquitous in nature and play an important role in the context of biology (networks of pacemaker cells in the heart), ecology (synchronously flashing fireflies and crickets that chirp in unison), even technological applications (arrays of lasers and microwave oscillators).

As has been eloquently described in a number of seminal references [16,17], Arthur T. Winfree was the first who considered, as early as 1967 [18], biological oscillators as phase oscillators, neglecting the amplitude, while in 1975 Yoshiki Kuramoto developed an analytical theory to explain synchronization of globally coupled phase oscillators of the form

$$\dot{\theta}_i = \omega_i + \frac{K}{N}\sum_{j=1}^{N}\sin(\theta_j - \theta_i), \quad i = 1 \ldots N \tag{7}$$

where K is a coupling constant and N represents the total number of oscillators (for a review of Kuramoto's theory see [19]). The frequencies $\omega_i \in g(\omega)$ are selected randomly from a natural frequency distribution, symmetric about Ω.

A truly surprising turn of events occurred in 2002, when Kuramoto and Battogtokh [20] studied the problem of $N \to \infty$ oscillators, as a reduction of the Complex Ginzburg-Landau equation for weak coupling:

$$\frac{\partial\theta(x,t)}{\partial t} = \omega - \int_0^1 G(x-x')\sin[\theta(x,t) - \theta(x',t) + \alpha]dx' \tag{8}$$

where ω is fixed, $\theta(x,t)$ is the phase of the oscillator at position x and time t, α is a time lag parameter and the kernel satisfies

$$G(x-x') \propto e^{-\kappa|x-x'|} \tag{9}$$

implying the presence of *non-local coupling* in the system. Solving this problem analytically as well as numerically (replacing $\theta(x,t)$ by $\theta_i(t)$ for large N) they observed a remarkable coexistence of coherent and incoherent oscillations in the form of a hybrid state shown in Fig. 6 under periodic boundary conditions.

Soon thereafter, Abrams and Strogatz [21,22] repeated the analysis using instead of (9) a cosine kernel

$$\frac{\partial\theta(x,t)}{\partial t} = \omega - \int_{-\pi}^{\pi} G(x-x')\sin[\theta(x,t) - \theta(x',t) + \alpha]dx' \tag{10}$$

$$G(x) = \frac{1}{2\pi}(1 + A\cos x), \quad 0 \le A \le 1 \tag{11}$$

which allowed them to solve the model explicitly. They noted that this state had never been seen in systems with local or global coupling and has nothing to do with partially locked or partially incoherent states that occur in populations of non-identical oscillators. They were the first who named it a "chimera state" and studied analytically its fundamental properties such as stability, dynamics and bifurcations. Indeed, what made the analysis possible was a remarkable ansatz by Ott and Antonsen [23], which permitted the reduction of the continuum model to a low-dimensional system of ordinary differential (odes) and showed that the appearance of a chimera could be viewed as the result of a saddle node bifurcation!

Thus, from what is known so far we may conclude the following: With local or global coupling, identical oscillators either synchronize or oscillate incoherently, but never do both simultaneously. However, under non-local coupling, identical oscillators can split into two coexisting synchronous and asynchronous domains, yielding what we called "chimera states".

Chimera states can also be found in networks of two coupled populations as shown in a case studied by [22], which can be written in the form:

$$\frac{d\theta_i^1}{dt} = \omega + \frac{\mu}{N}\sum_{N}^{j=1}\sin(\theta_j^1 - \theta_i^1 - \alpha) + \frac{\nu}{N}\sum_{N}^{j=1}\sin(\theta_j^2 - \theta_i^1 - \alpha) \tag{12}$$

$$\frac{d\theta_i^2}{dt} = \omega + \frac{\mu}{N}\sum_{N}^{j=1}\sin(\theta_j^2 - \theta_i^2 - \alpha) + \frac{\nu}{N}\sum_{N}^{j=1}\sin(\theta_j^1 - \theta_i^2 - \alpha) \tag{13}$$

where the coupling between populations $\nu > 0$ is somewhat smaller than the coupling $\mu > 0$ within each population. Interestingly, such two-population chimeras have been also been recently found in mechanical systems of pendulum-like oscillators [38], as we discuss in more detail in Sect. 4 below.

3.2 Chimera states in the context of neuroscience

Many birds as well as dolphins sleep with one eye open, in the sense that one hemisphere of the brain may be considered synchronous while the other is asynchronous. This coexistence of synchrony and asynchrony is what we referred to as a chimera state.

In this context, J. Hizanidis at al. [24] were the first to study a network of 2-Dimensional (2D) Hindmarsh-Rose (HR) models of neuron oscillators described by the equations

$$\dot{x}_k = y_k - x_k^3 + 3x_k^2 + J + \frac{\sigma_x}{2R}\sum_{j=k-R}^{j=k+R}[b_{xx}(x_j - x_k) + b_{xy}(y_j - y_k)] \tag{14}$$

$$\dot{y}_k = 1 - 5x_k^2 - y_k + \frac{\sigma_y}{2R}\sum_{j=k-R}^{j=k+R}[b_{yx}(x_j - x_k) + b_{yy}(y_j - y_k)]. \tag{15}$$

The above pair of equations assigned to each node was introduced by Hindmarsh and Rose [25] to describe a single neuron in terms of an x(t) variable that describes the potential across the neuron membrane and a y(t) variable representing the ion currents flowing across the membrane. In the above system the parameter J is introduced to denote an externally applied current, while the coupling of each oscillator

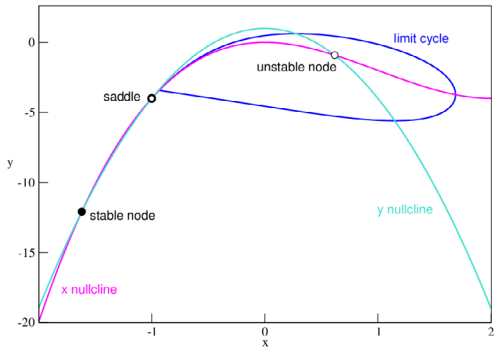

Fig. 7. Phase space analysis of the solutions of the 2D HR model in the plane, at $J = 0$.(Figure taken from [24].)

to its R neighbors involves, in general, interactions between both x and y variables of the oscillators given by the elements of a matrix B

$$B = \begin{pmatrix} b_{xx} & b_{xy} \\ b_{yx} & b_{yy} \end{pmatrix} = \begin{pmatrix} cos\phi & sin\phi \\ -sin\phi & cos\phi \end{pmatrix}$$

as suggested in [34].

A simple analysis of the 2D HR model in the x-y phase plane presented in Fig. 7 reveals a case of *bistability*, where a stable node and a stable limit cycle (to which different neuron oscillators can be attracted) are simultaneously present. As is also evident, an unstable node and a saddle point are present in the dynamics at $J = 0$. This bistability phenomenon at $J = 0$ is evident in the behavior of the full system as seen in the top panel of Fig. 8, where many asynchronous oscillators appear interspersed among the synchronous ones, when the coupling is diagonal with $\phi = -\pi$ in the coupling matrix B.

As shown by the second row of panels in Fig. 8 complete synchronization may also be achieved by choosing $\phi = \pi/4$. Chimeras are discovered when the coupling in (14) is restricted to the x-terms (i.e $\phi = 0$), and are split in two or three parts as the bottom two panels in Fig. 8 demonstrate. Now, as the external current J is increased, the two nodes in Fig. 7 coalesce at the saddle point via a saddle node bifurcation and the limit cycle is left as the only attractor. In that case, gradually increasing the coupling constant $\sigma_x = \sigma$ and keeping $\sigma_2 = 0$, it is possible discover the chimera shown in the left panels of Fig. 9. Note that this occurrence is accompanied by a gradual collapse of the limit cycle, as indicated by the right panels of Fig. 9.

Next, the authors of [24] turned to an analogous study of the dynamics of 3D HR models, in which every neuron is described by three first order odes [26]

$$\dot{x} = -ax^3 + bx^2 + y - z + J \tag{16}$$

$$\dot{y} = c - dx^2 - y$$

$$\dot{z} = r(s(x - x_0) - z) \tag{17}$$

where $s = 4, x_0 = -1.6, a = 1, b = 3, c = 1, d = 5, r = 0.001$, x denotes again the membrane potential, y describes the activity of fast gated ion channels (Na^+ and K^+), and z represents the activity of slow gated ion channels (Ca^+ and Cl^-). The interesting feature of these equations, unlike the 2D model, is that their solutions can exhibit bursting and spiking patterns (see Fig. 10) commonly observed in realistic neurons.

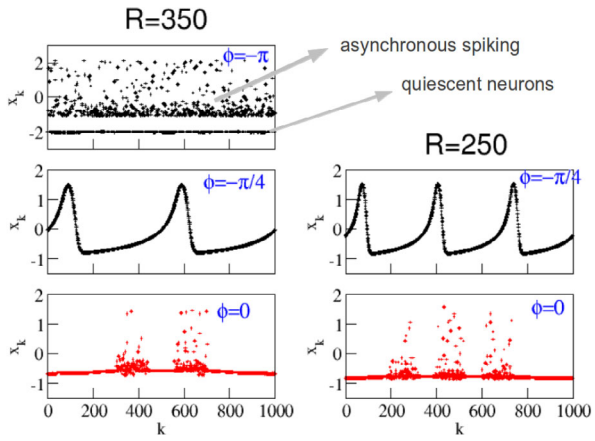

Fig. 8. Snapshots of the x_k variables at $t = 3000$, $N = 1000$, $\sigma_x = \sigma_y = 0.1$, $J = 0$, as the range R and the angle ϕ of the coupling matrix are varied. Chimeras were only found for diagonal coupling as shown in the bottom two panels. (Figure taken from [24].)

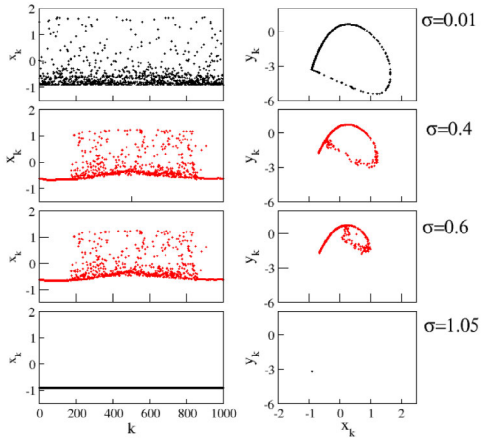

Fig. 9. Snapshots of the x_k variables at $R = 350$, $N = 1000$, $\sigma_x = \sigma$ and $\sigma_y = 0$, at $J > 0$, as the value of σ is varied. Single chimeras were found to be associated with a collapse of the limit cycle oscillations of each neuron. (Figure taken from [24].)

Searching for chimeras, J. Hizanidis et al. [24] examined a network of N=1000 3D-HR oscillators described by the equations

$$\dot{x}_k = y_k - {x_k}^3 + b{x_k}^2 + J - z_k + \frac{\sigma_x}{2R} \sum_{j=k-R}^{j=k+R} (x_j - x_k)$$

$$\dot{y}_k = 1 - 5{x_k}^2 - y_k$$

$$\dot{z}_k = r(s(x_k + 1.6) - z_k, \quad k = 1, 2, ..., N,$$

where again only x to x coupling is assumed, $s = 4$ adjusts firing frequency adaptation and burst production, $r = 0.01$ is the spiking frequency (i.e. number of spikes per bursting) and b and J are parameters affecting the transition between spiking and bursting. Interestingly, as shown in Fig. 10, chimeras were found to exist in this case at coupling constant values about $\sigma = 0.5$, when both bursting and spiking behavior

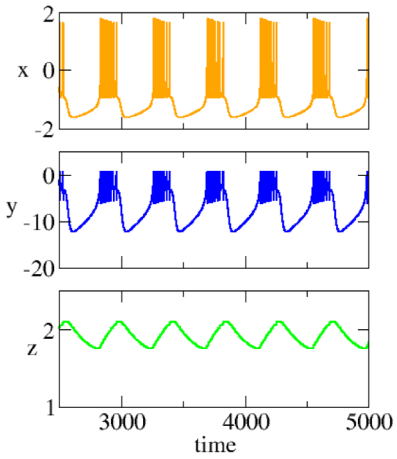

Fig. 10. Chimeras are observed in the 3D HR network model as the coupling constant increases and both bursting and spiking are present in the x(t) oscillations. Here $b = 3$ and $J = 5$. (Figure taken from [24].)

are present in the x(t) oscillations. This suggests that chimeras may indeed be found to exist one day in realistic experiments of interest to neuroscience.

Extending this study to two-population networks of 2D HR neuron oscillators, we may now proceed to solve the following systems of equations

$$\begin{aligned}
\dot{x}_k^1 &= y_k^1 - (x_k^1)^3 + 3(x_k^1)^2 + J + \frac{\sigma}{N}\sum_{j=1}^{N}(x_j^1 - x_k^1) + \frac{\rho}{N}\sum_{j=1}^{N}(x_j^2 - x_k^1) \\
\dot{y}_k^1 &= 1 - 5(x_k^1)^2 - y_k^1 \\
\dot{x}_k^2 &= y_k^2 - (x_k^2)^3 + 3(x_k^2)^2 + J + \frac{\sigma}{N}\sum_{j=1}^{N}(x_j^2 - x_k^2) + \frac{\rho}{N}\sum_{j=1}^{N}(x_j^2 - x_k^1) \\
\dot{y}_k^2 &= 1 - 5(x_k^2)^2 - y_k^2
\end{aligned} \tag{18}$$

building on the experience we have accumulated from the one population case. In other words, we consider again only coupling in the x- variable and ask how does the above system of two ring networks behave under all-to-all coupling when we vary the current J and the coupling parameter ρ. Will we observe chimeras in this case?

For small internal coupling $\sigma = 0.1$ within each network the two populations remain unsynchronized, as the inter-network coupling increases from $\rho = 0.01$ to 0.1, with $R = 340$, $b = 3$ and $J = 5$. As Fig. 11 demonstrates, however, for larger internal coupling $\sigma = 0.5$, as the inter network coupling increases from $\rho = 0.01$ in (a) to 0.1 in (j) ($R = 340$, $b = 3, J = 5$) chimera states indeed appear!

4 Chimeras in two coupled populations of pendulum-like oscillators

Let us now consider a two population network of non-identical phase oscillators in the form studied in [27,28,36,37] and extend it by introducing an inertial term proportional to a mass parameter $m > 0$. We thus obtain a network of two populations of pendulum-like elements with all-to-all coupling within (and between) the populations,

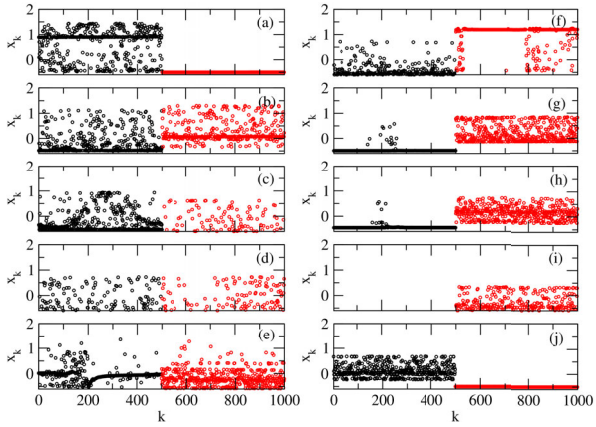

Fig. 11. For internal coupling parameter $\sigma = 0.5$, as the inter-network coupling increases from $\rho = 0.01$ in (a) to 0.1 in (j) chimera states appear (R = 340, $b = 3, J = 5$.)

governed by the *second order* odes:

$$m\frac{d^2\theta_i^1}{dt^2} + \epsilon\frac{d\theta_i^1}{dt} = \omega_i - d_1 sin(\theta_i^1) + \frac{\mu}{N}\sum_{j=1}^{N}\sin(\theta_j^1 - \theta_i^1 - \alpha) + \frac{\nu}{N}\sum_{j=1}^{N}\sin(\theta_j^2 - \theta_i^1 - \alpha) \tag{19}$$

$$m\frac{d^2\theta_i^2}{dt^2} + \epsilon\frac{d\theta_i^2}{dt} = \omega_i - d_2 sin(\theta_i^2) + \frac{\mu}{N}\sum_{j=1}^{N}\sin(\theta_j^2 - \theta_i^2 - \alpha) + \frac{\nu}{N}\sum_{j=1}^{N}\sin(\theta_j^1 - \theta_i^2 - \alpha) \tag{20}$$

where $i, j = 1, ...N$, N is the number of oscillators in each population (subnetwork). The two populations are labeled by the superscripts 1 and 2, while $\mu > 0$ and $\nu >$ are fixed positive parameters representing the coupling strength within the same population and between the two populations respectively. The ω_i are taken from a Lorentzian distribution $g(\omega)$ [27], while μ and ν satisfy $\mu + \nu = 1$, with $\mu > \nu$ as in [28]. The oscillators in population 1 are numbered 1 to 500, while those in population 2 from 501 to 1000.

Note that Eqs. (19) and (20) describe the motion of two subnetworks of pendulum-like oscillators, with each pendulum characterized by a mass m and a damping parameter ϵ. In what follows, we first neglect gravity, setting $d_1 = d_2 = 0$ in (19) and (20) and later allow these parameters to be non-zero.

Now, as chimera states represent *attractors* of the dynamics, one does not expect that they exist in the conservative limit $\epsilon = 0$. Thus, in [38] the authors attempted to locate chimeras in two ways: (a) First they set $\epsilon = 1$ and increased the value of m gradually from 0 and (b) they fixed m at a value where a chimera state is observed and investigated the range of decreasing $\epsilon < 1$ values over which the phenomenon persists.

Following [38], let us set $N = 500$, $\mu = 0.6$, $\nu = 0.4$, $\alpha = \pi/2 - 0.05$ and use the Lorentzian distribution $g(\omega) = \frac{1}{\pi}\frac{\gamma}{\gamma^2+\omega^2}$ with $\gamma = 0.001$. Varying the α value one discovers chimeras very close to $\alpha = \pi/2 - 0.05$. Moreover, with $\mu = 0.6$, chimeras cease to exist for inter-population coupling $0 < \nu < 0.3$.

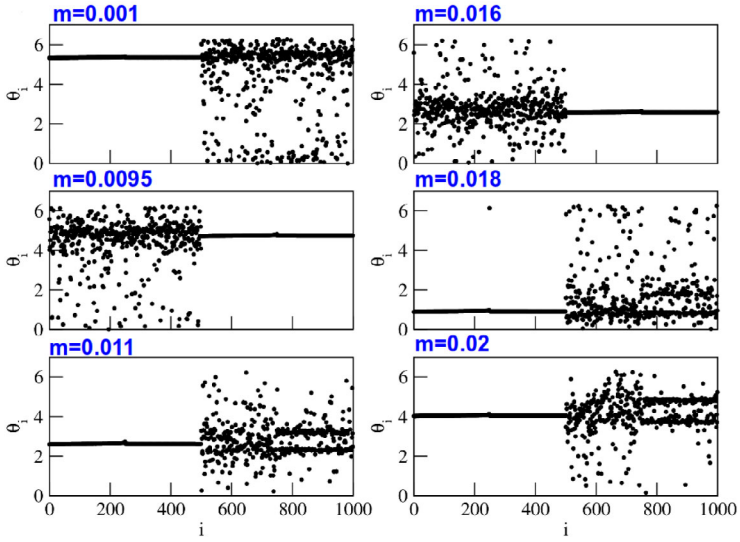

Fig. 12. Snapshots of the variable θ_i for both populations at $t = 3000$, $\epsilon = 1$ and increasing mass values: (a) $m = 0.001$, (b) $m = 0.0095$, (c) $m = 0.011$, (d) $m = 0.016$, (e) $m = 0.018$, and (f) $m = 0.02$. Gravity is neglected, taking $d_i = 0, i = 1, 2$ in Eqs. (19) and (20). (Figure taken from Ref. [38].)

4.1 A threshold for the onset of chimeras in the m, ϵ plane

In [38] the authors first investigated the emergence of chimeras by increasing the mass m above 0, keeping all other parameters constant. Setting $\epsilon = 1$ and $d_1 = d_2 = 0$, they demonstrated that chimera states are found to exist over a narrow interval of mass values $0 < m \approx 0.02$, as shown in Fig. 12. They also noted that these results do not change significantly when $d_i > 0, i = 1, 2$ and gravity is taken into account in Eqs. (19), (20).

Let us now ask what happens when ϵ is decreased, for a mass value at which chimeras have been found to exist. For example, let us take $m = 0.011$ (see Fig. 12) and start decreasing $0 \leq \epsilon \leq 1$. What one observes is that at this m value chimeras persist down to approximately $\epsilon = 0.61$. Below this threshold value chimeras are no longer observed and only patterns of nearly synchronized subgroups appear in the network.

Repeating these calculations for different values of m and estimating approximate thresholds ϵ_{th}) in the $(m, \epsilon(m)$ plane below which chimera states break down, it was found in [38] that these thresholds fall on a nearly straight line, as seen in Fig. 13, for $m = 0.011$ and decreasing damping rates: (a) $\epsilon = 1$, (b) $\epsilon = 0.9$, (c) $\epsilon = 0.68$, and (d) $\epsilon = 0.56$.

4.2 Chimera explanation by reduction to a single pendulum equation

How can we explain these pendulum chimeras in a qualitative way? An attempt in this direction was made in [38] by first simplifying the notation in Eqs. (19) and (20) by calling the angle variables in the first and second population as $\theta_i^1 \equiv \phi_i$ and $\theta_i^2 \equiv \theta_i$ respectively. Next, a typical chimera at $m = 0.011$ and $\epsilon = 1$ is considered (see Fig. 12), in which the second population is synchronized and the first is asynchronous. Thus, taking $d_1 = d_2 = 0$ and $\omega_i = \omega$ the variables of the synchronized population

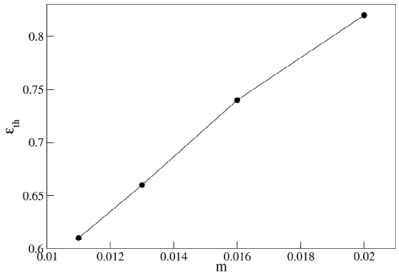

Fig. 13. Setting $m = 0.011, 0.013, 0.016, 0.02$ and plotting the corresponding $\epsilon(m) = 0.61, 0.66, 0.74, 0.82$ values in the (m, ϵ_{th}) plane, threshold values $\epsilon_{th} = \epsilon(m)$ are determined below which chimeras cease to exist. Note that $\epsilon(m)$ increases nearly linearly as a function of the mass m. (Figure taken from Ref. [38].)

can be equated to a single $\theta(t)$ obeying the equation:

$$m\frac{d^2\theta}{dt^2} + \epsilon\frac{d\theta}{dt} = \omega - \mu\sin(\alpha) + \frac{\nu}{N}\sum_{j=1}^{N}\sin(\phi_j - \theta - \alpha), \tag{21}$$

in which the quantity $\omega - \mu\sin(\alpha)$ on the right hand side is a constant average about which $\theta(t)$ oscillates.

Expanding now the sine in the sum appearing in (21) yields two terms which can be expressed in terms of quantities averaged over the oscillations of the unsynchronized population as follows:

$$s(t) = \frac{1}{N}\sum_{j=1}^{N}\sin(\phi_j), \quad c(t) = \frac{1}{N}\sum_{j=1}^{N}\cos(\phi_j), \tag{22}$$

so that Eq. (21) finally becomes

$$m\frac{d^2\theta}{dt^2} + \epsilon\frac{d\theta}{dt} = \omega - \mu\sin(\alpha) + \nu s(t)\cos(\theta) - \nu c(t)\sin(\theta), \tag{23}$$

where the variable $\theta \to \theta - \alpha$ has been shifted to θ without loss of generality.

As noted in [38], the above analysis is motivated by the the numerical observation that the asynchronous variables oscillate on the average with the same period as the synchronous ones, as seen in Fig. 14. Remarkably these quantities have the same period as the original variables, suggesting that the chimera state represents a phenomenon of entrainment due to periodic forcing. This is indeed verified by the fact that the oscillatory terms $s(t)$ and $c(t)$, which represent the effect of the incoherent population, enter parametrically in Eq. (23).

It is remarkable that the amplitude and form of the $\theta(t)$ oscillations are clearly related to the corresponding quantities of the actual $\theta_i(t)$ oscillations shown in Fig. 15. Note, however, that there is a certain "deformation" in the oscillations of the reduced variable and a slightly smaller period than the one of the full system, which may be due to the imposed simplifications and need to be better understood. Nevertheless, we find it quite interesting that the above severe reduction of the problem to a single damped pendulum Eq. (23) has allowed us to propose a plausible qualitative explanation of such a complex phenomenon as the chimera state of a two-population network of pendulum-like oscillators.

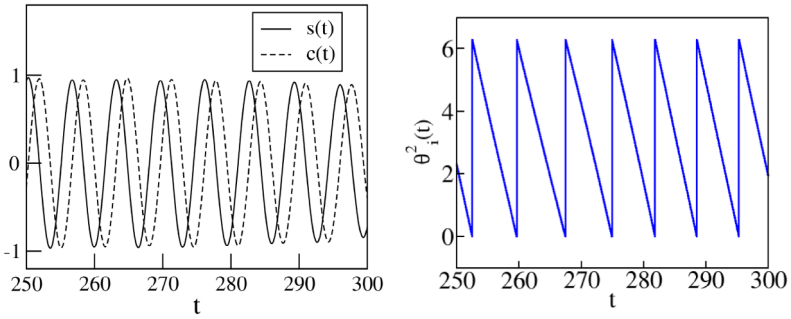

Fig. 14. a) The averaged variables $s(t)$ (solid line) and $c(t)$ (dashed line) oscillate with the same period as (b) the solution $\theta(t)$ of Eq. (23). The parameter values here are $m = 0.011$ and $\epsilon = 1$. (Figure taken from Ref. [38].)

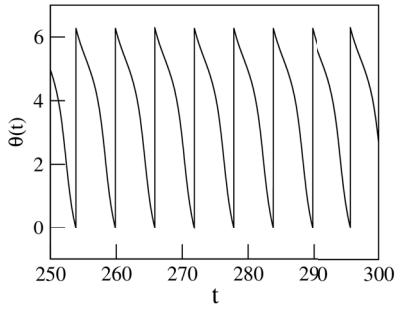

Fig. 15. The solution of the single pendulum equation Eq. (23) (left) approximates very well the oscillation of the synchronized variables $\theta_i(t)$ as computed from Eq. (20), for $\omega_i = \omega$, $m = 0.011$ and $\epsilon = 1$. (Figure taken from Ref. [38].)

5 Discussion and conclusions

Many complex phenomena from physics to biology are modeled by networks of coupled nonlinear oscillators, which are mathematically expressed by appropriate systems of first order odes. These phenomena are called complex because, even though at the level of few oscillators (or nodes) their time evolution is well understood, when large numbers of nodes are involved, they often display surprising properties and unexpected global behavior.

In the study of these problems, one starts by assuming that the given equations of motion correctly describe the dynamics of each individual node. The reasons, therefore, why the system as a whole behaves in an unexpected way must be sought in the details of the coupling between the different variables of the system, often described also as the connectivity pattern of the network.

In this review, I have examined only one aspect of this connectivity, focusing on the *range* of the interactions among the nodes of the network. The specific question I have asked is in what way does this range affect the global oscillatory dynamics of the system. More specifically, I have chosen two situations: One regarding the distinction between what I called "weak" and "strong" chaos in 1-dimensional lattices of Hamiltonian mechanics and one related to the emergence of the so-called "chimera states" of coexisting synchronous and asynchronous populations in biological networks of neuron oscillators.

In the case of Hamiltonian oscillators, we discovered that if we couple all particle pairs by terms proportional to $r^{-\alpha}$, where $r = |x_i - x_j|$ is their mutual distance,

the dynamics and statistics of the system crucially depends on whether the positive parameter α satisfies $1 < \alpha < \infty$ or $0 \leq \alpha \leq 1$. The first case corresponds to *short range interactions* and is characterized by *strong chaos*, as in the thermodynamic limit (of increasing energy E and number of particles N with E/N fixed) Lyapunov exponents grow and Boltzmann Gibbs statistics prevails. On the other hand, in the second case of *long range interactions*, taking the thermodynamic limit, we find that Lyapunov exponents decrease and the statistics becomes of Tsallis type characterizing what we call *weak chaos*.

Turning now to our biological networks of coupled neuron oscillators of the Hindmarsh-Rose type, we showed that these remarkable chimera states of coexisting synchronous and asynchronous oscillating sub-networks are critically affected by the presence of of long range interactions. For example, in ring networks the very occurrence of chimeras depends on the number R of left and right neighbors of each one of the N oscillators, where N and R are sufficiently large. Thus, keeping all interaction factors equal (usually $1/N$ for each nodal pair), all we have to do is vary the coupling strengths between variables (within each sub-network and between sub-networks) and we will witness the birth and death of chimeras in a great variety of examples. In fact, one does not have to limit oneself to biological oscillators. As I showed using specific examples in this review, one can follow the above protocol and observe analogous chimera states in sub-populations of mechanical networks of pendulum-like oscillators, as long as one chooses appropriate coupling constants and pair interactions that are sufficiently long range.

I would like to close with some comments regarding the potential applications of the results described above as well as those obtained by other researchers using similar mathematical models. In the realm of mechanics, energy transport in molecular lattices has already produced interesting discoveries which have started to be observed in experiments particularly in disordered media. On the other hand, mechanical pendulum systems were among the first where the occurrence of chimera states was experimentally verified. Regarding real biological systems, the quest for the laboratory observation of chimera states is actively pursued at several research centers around the world. The difficulty here, of course, is that when one deals with live neuron systems whose dynamics continually changes, chimera states are expected to be metastable and hence short lived. However, even if they are rare to find, their ubiquity in mathematical models is very encouraging and has alerted us to new exciting phenomena that may possibly contribute to our deeper understanding of neuron dynamics.

Finally, it is worth noting that very recently Hindmarsh-Rose models have been used to study the dynamics on the exactly known neural network of the *C.elegans* worm [39]. Even though the true equations of motion connecting the neurons of the *C.elegans* are not known, the exact neural network was seen to consist of six sub-networks, many of which had similar regimes of synchronization in the plane of coupling parameters of the system. Remarkably, at the boundaries of these regimes, integrated information estimates are highest and evidence of the occurrence of chimera states is observed [39,40]. We may, therefore, conclude that the era of exciting research in the mathematical modelling of brain dynamics is currently entering a new and very fascinating stage.

I am very grateful to a great number of colleagues and collaborators for teaching me the importance of long range interactions in physical systems and the significance of chimera states in biological networks, while working closely with me to produce the results reviewed in this paper. In the former group I mention Constantino Tsallis, Chris Antonopoulos and Eleni Christodoulidi and in the latter Tassos Bezerianos, Ioanna Hizanidis and Vassilis Kanas. Regarding the support we have all received to carry out the papers summarized in this

review, I gratefully acknowledge that this research has been co-financed by the European Union (European Social Fund – ESF) and Greek national funds through the Operational Program "Education and Lifelong Learning" of the National Strategic Reference Framework (NSRF) – Research Funding Program: Thales. Investing in knowledge society through the European Social Fund.

References

1. A.J. Lichtenberg, M.A. Lieberman, *Regular and Chaotic Dynamics*, Applied Mathematical Sciences, Vol. 38 (Springer, 1992)
2. G.P. Berman, F.M. Izrailev, Chaos **15**, 015104 (2005)
3. Ch. Antonopoulos, T. Bountis, V. Basios, Physica A **390**, 3290 (2011)
4. T. Bountis, H. Skokos, *Complex Hamiltonian Dynamics*, Springer Synergetics series (Springer, Berlin, 2012)
5. M. Antoni, S. Ruffo, Phys. Rev. E **52**, 2361 (1995)
6. V. Latora, A. Rapisarda, S. Ruffo, Phys. Rev. Lett. **80**, 692 (1998)
7. C. Anteneodo, C. Tsallis, Phys. Rev. Lett. **80**, 5313 (1998)
8. T. Dauxois, V. Latora, A. Rapisarda, S. Ruffo, A. Torcini, edited by T. Dauxois, S. Ruffo, E. Arimondo, M. Wilkens, Lect. Notes Phys. **602**, 458 (2002)
9. V.E. Tarasov, G.M. Zaslavsky, Commun. Nonlinear Sci. Numer. Simul. **11**, 885 (2006)
10. K.A. Takeuchi, H. Chaté, F. Ginelli, A. Politi, A. Torcini, Phys. Rev. Lett. **107**, 124101 (2011)
11. F. Ginelli, K.A. Takeuchi, H. Chaté, A. Politi, A. Torcini, Phys. Rev. E **84**, 066211 (2011)
12. Th. Manos, S. Ruffo, Trans. Theor., Stat. Phys. **40**, 360 (2011)
13. H. Christodoulidi, C. Tsallis, T. Bountis, EPL **108**, 40006 (2014)
14. C. Tsallis, *Introduction to Nonextensive Statistical Mechanics: Approaching a Complex World* (Springer, New York, 2009)
15. H. Christodoulidi, T. Bountis, C. Tsallis, L. Drossos, Chaotic behavior of the Fermi–Pasta–Ulam β–model with different ranges of particle interactions (submitted) (2015)
16. A. Pikovsky, M. Rosenblum, J. Kurths, *Synchronization – A Universal Concept in Nonlinear Sciences* (Cambridge University Press, 2001)
17. S. Boccaletti, J. Kurths, G.V. Osipov, D. Valladares, C. Zhou Phys. Rep. **366**, 1 (2002)
18. A.T. Winfree, J. Theor. Biol. **28**, 327374 (1967)
19. J.A. Acebron, L.L. Bonilla, C.J. Pérez Vicente, F. Ritort, R. Spigleri, Rev. Mod. Phys. **77**, 138 (2005)
20. Y. Kuramoto, D. Battogtokh, Nonlin. Phen. Complex Sys. **5**, 380 (2002)
21. D.M. Abrams, S.H. Strogatz, Phys. Rev. Lett. **93**, 174102 (2004)
22. D.M. Abrams, R. Mirollo, S. Strogatz, D.A. Wiley, Phys. Rev. Lett. **101**, 084103 (2008)
23. E. Ott, T.M. Antonsen, Chaos **18**, 037113 (2008)
24. J. Hizanidis, V.G. Kanas, A. Bezerianos, T. Bountis, Int. J. Bif. Chaos **24**, 1450030 (2014)
25. J.L. Hindmarsh, R.M. Rose, Nature, Lond. **296**, 162 (1982)
26. J.L. Hindmarsh, R.M. Rose, Proc. R. Soc. London, Ser. B **221**, 87 (1984)
27. C.R. Laing, Phys. Rev. E **81**, 066221 (2010)
28. C.R. Laing, K. Rajendran, I.G. Kevrekidis, Chaos **22**, 013132 (2012)
29. I. Omelchenko, Y.L. Maistrenko, P. Hövel, E. Schöll, Phys. Rev. Lett. **106**, 234102 (2011)
30. M.R. Tinsley, S. Nkomo, K. Showalter, Nat. Phys. **8**, 662 (2012)
31. A.M. Hagerstrom, E. Thomas, R. Roy, P. Hövel, I. Omelchenko, E. Schöll, Nat. Phys. **8**, 658 (2012)
32. N.C. Rattenborg, C.J. Amlaner, S.L. Lima, Neurosci. Biobehav. Rev. **24**, 817 (2000)
33. C.G. Mathews, J.A. Lesku, S.L. Lima, C.J. Amlaner, Ethology **112**, 286 (2006)
34. I. Omelchenko, O.E. Omel'chenko, P. Hövel, E. Schöll, Phys. Rev. Lett. **110**, 224101 (2013)

35. E.A. Martens, S. Thutupalli, A. Fourriére, O. Hallatschek, Proc. Natl. Acad. Sci. **110**, 10563 (2013)
36. C.R. Laing, Chaos **19**, 013113 (2009)
37. C.R. Laing, Chaos **22**, 043104 (2012)
38. T. Bountis, V.G. Kanas, J. Hizanidis, A. Bezerianos, Eur. Phys. J. Special Topics **223**, 721 (2014)
39. C.G. Antonopoulos, A.S. Fokas, T. Bountis, Eur. Phys. J. Special Topics **225**, 1255 (2016)
40. J. Hizanidis, N. Kouvaris, G. Zamora-Lopéz, A. Díaz-Guilera, Ch. Antonopoulos, Chimera-like dynamics in modular neural networks, Scientific Reports **6**, 19845 (2016)